Cyanate Intercalation in Nickel Hydroxide

Bora Mavis and Mufit Akinc*

Ames Laboratory and Materials Science and Engineering Department, 2220 Hoover Hall, Iowa State University, Ames, Iowa 50011-2300

Received December 30, 2005. Revised Manuscript Received August 31, 2006

α-$Ni(OH)_2$ and Ni−Al layer double hydroxides (LDHs) precipitated by urea were investigated with FTIR and XPS. Possible modes of cyanate (CNO^-) coordination during the nucleation and growth of precipitates is discussed. In the early stages, cyanate ion in α-$Ni(OH)_2$ is found mainly to be N-bonded to Ni^{2+} ions in the layers, whereas later in the growth stages, it is bonded through oxygen. In LDHs cyanate remains N-bonded. These changes in the coordinations modes are related to the decreasing supersaturation levels during digestion. XPS results support the FTIR results.

Introduction

Nickel hydroxides are used in rechargeable batteries and are prepared from aqueous solutions. $Ni(OH)_2$ is the common positive electrode for nickel-based alkaline secondary batteries.[1] It has two polymorphic forms, β and α. The β phase exhibits closely packed brucite type layers in which Ni^{2+} is in the center of hydroxyl octahedra, whereas α phase exhibits larger layer separations afforded by the intercalation of water and anions.[2] Of the two phases, α has been the main point of interest. Mainly due to the high difference in oxidation state between the reduced hydrated hydroxide and the oxidized form (γ phase usually), a higher specific capacity is anticipated in α. However, stability of α against transformation into β in its strongly alkaline electrolyte (generally 6 M KOH) during cycling or storage has been a long-lasting problem.[1,3,4]

Urea decomposition at temperatures above 60 °C has been widely applied to produce various precursors for mixed metal oxides.[5−7] Homogeneous precipitation forced by urea decomposition in solutions containing Ni^{2+} ions has been observed to yield α-$Ni(OH)_2$.[8−17] Nevertheless, the product does not show stability against transformation into β in alkaline solutions. The intercalating species besides water were found to be either cyanate (intermediate decomposition product) or carbonaceous species.[11,14,17−19]

It was reported that α phase could be stabilized by trivalent cation substitution for Ni^{2+}. Substitution of trivalent cations (such as Al^{3+}, Cr^{3+}, Co^{3+}, Mn^{3+}, and Fe^{3+}) creates a positive charge in the sheets, and insertion of hydrated anions between the layers is believed to compensate this extra charge.[20−23] Layer double hydroxides (LDHs) are a class of intercalation

* Corresponding author e-mail: makinc@iastate.edu.

(1) Faure, C.; Delmas, C.; Fouassier, M. Characterization of a turbostratic α-nickel hydroxide quantitatively obtained from an nickel sulfate solution. *J. Power Sources* **1991**, *35* (3), 279−90.
(2) Rajamathi, M.; Kamath, P. V.; Seshadri, R. Polymorphism in nickel hydroxide: Role of interstratification. *J. Mater. Chem.* **2000**, *10* (2), 503−6.
(3) Braconnier, J. J.; Delmas, C.; Fouassier, C.; Figlarz, M.; Beaudouin, B.; Hagenmuller, P. A novel nickel(II) hydroxide obtained by soft chemistry. *Rev. Chim. Miner.* **1984**, *21* (4), 496−508.
(4) Kamath, P. V.; Subbanna, G. N. Electroless nickel hydroxide: synthesis and characterization. *J. Appl. Electrochem.* **1992**, *22* (5), 478−82.
(5) Sordelet, D.; Akinc, M. Preparation of spherical, monosized yttrium oxide precursor particles. *J. Colloid Interface Sci.* **1988**, *122* (1), 47−59.
(6) Sordelet, D. J.; Akinc, M.; Panchula, M. L.; Han, Y.; Han, M. H. Synthesis of yttrium aluminum garnet precursor powders by homogeneous precipitation. *J. Eur. Ceram. Soc.* **1994**, *14* (2), 123−30.
(7) Soler-Illia, G. J. d. A. A.; Jobbagy, M.; Candal, R. J.; Regazzoni, A. E.; Blesa, M. A. Synthesis of metal oxide particles from aqueous media: the homogeneous alkalinization method. *J. Dispersion Sci. Technol.* **1998**, *19* (2 & 3), 207−28.
(8) Akinc, M.; Jongen, N.; Lemaitre, J.; Hofmann, H. Synthesis of nickel hydroxide powders by urea decomposition. *J. Eur. Ceram. Soc.* **1998**, *18* (11), 1559−64.
(9) Widjaja, A. Synthesis and characterization of nickel hydroxide powders for battery applications. M.Sc. Thesis, Iowa State University, Ames, IA, 1997.
(10) Yazdi, I. Synthesis and electrochemical studies of cobalt substituted nickel hydroxide for battery applications. M.Sc. Thesis, Iowa State University, Ames, IA, 1999.
(11) Maruthiprasad, B. S.; Sastri, M. N.; Rajagopal, S.; Seshan, K.; Krishnamurthy, K. R.; Rao, T. S. R. P. A novel nickel trihydroxy isocyanate−preparation and characterization. *Proc. Indian Acad. Sci., Chem. Sci.* **1988**, *100* (6), 459−62.
(12) Avena, M. J.; Vazquez, M. V.; Carbonio, R. E.; De Pauli, C. P.; Macagno, V. A. A simple and novel method for preparing $Ni(OH)_2$. Part I: Structural studies and voltammetric response. *J. Appl. Electrochem.* **1994**, *24* (3), 256−60.
(13) Torresi, R. M.; Vazquez, M. V.; Gorenstein, A.; Torresi, S. I. C. D. Infrared characterization of electrochromic nickel hydroxide prepared by homogeneous chemical precipitation. *Thin Solid Films* **1993**, *229* (2), 180−6.
(14) Dixit, M.; Subbanna, G. N.; Kamath, P. V. Homogeneous precipitation from solution by urea hydrolysis: a novel chemical route to the α-hydroxides of nickel and cobalt. *J. Mater. Chem.* **1996**, *6* (8), 1429−32.
(15) Jobbagy, M.; Soler-Illia, G. J. D. A. A.; Regazzoni, A. E.; Blesa, M. A. Synthesis of copper(II)-containing nickel(II) hydroxide particles as precursors of copper(II)-substituted nickel(II) oxides. *Chem. Mater.* **1998**, *10* (6), 1632−7.
(16) Soler-Illia, G. J. D. A. A. A study of Cu-Ni and Cu-Zn mixed oxide precursors synthesis by homogeneous alkalinization methods. Ph.D. Thesis, Universidad de Buenos Aires, Buenos Aires, Argentina,1998.
(17) Soler-Illia, G. J. d. A. A.; Jobbagy, M.; Regazzoni, A. E.; Blesa, M. A. Synthesis of nickel hydroxide by homogeneous alkalinization. Precipitation mechanism. *Chem. Mater.* **1999**, *11* (11), 3140−6.
(18) Mavis, B.; Akinc, M. Kinetics of urea decomposition in the presence of transition metal ions: Ni^{2+}. *J. Am. Ceram. Soc.* **2006**, *89* (2), 471−7.
(19) Mavis, B.; Akinc, M. Details of urea decomposition in the presence of transition metal ions. *Ceram. Eng. Sci. Proc.* **2003**, *24* (3), 117−22.
(20) Faure, C.; Delmas, C.; Fouassier, M.; Willmann, P. Preparation and characterization of cobalt-substituted α-nickel hydroxides stable in potassium hydroxide medium. Part I. α′-Hydroxide with an ordered packing. *J. Power Sources* **1991**, *35* (3), 249−61.

10.1021/cm0528835 CCC: $33.50
Published on Web 10/12/2006

compounds that are represented by the general formula $[M^{2+}_{1-x}M^{3+}_{x}(OH)_2]^{x+}[A^{n-}_{x/n}]^{x-}\cdot mH_2O$. Stabilization of α-Ni(OH)$_2$ might be investigated under this class of materials (i.e., LDHs).[24] Costantino et al. had investigated synthesis of Mg−Al, Ni−Al, and Zn−Al LDHs with urea and reported that Mg−Al crystals could be refined by the Rietveldt method.[25] However, they assumed that all the intercalated species would be water and carbonate without any spectroscopic evidence.

Soler-Illia et al. mentioned presence of cyanate ion in the precipitates.[7] Their model, which did not include metal ions, predicted that cyanate accumulates in the initial stages of hydrolysis. A more comprehensive model, which includes Ni^{2+} leading to precipitation, hydrolysis, and complexation reactions, is necessary for a complete description of the precipitation process. Indeed, we have shown that nickel cyanate complexes were the dominant species prior to nucleation stage.[18,19,26]

Concurrent to this work, a number of articles have appeared on the use of urea hydrolysis for the synthesis of Ni-based LDHs.[27−30] Shu et al. have prepared a Ni(II)/Ti(IV) LDH (Ni−Ti LDH) utilizing urea hydrolysis. The intercalation of cyanate ions can be confirmed through visual inspection of the FTIR spectra acquired from powders resulting from digestion times longer than 1.5 h.[27] However, a detailed analysis on the changing peak profiles was not carried out.

Here we will elaborate on spectral features observed in α-Ni(OH)$_2$ and Ni−Al LDHs produced by urea decomposition. Cyanate in metal−cyanate complexes was generally reported to be N-bonded to the metal.[31−36] Forster et al.[35] studied nickel isocyanate complexes and reported an intense peak at 2186 cm^{-1} with a shoulder at 2237 cm^{-1}. This combined with our observation of an intense peak at 2250 cm^{-1} with a low wavenumber shoulder for the α phase and an intense peak at ≈2186 cm^{-1} with a high wavenumber shoulder for the LDHs was intriguing. Carbacho et al. reported an interesting change in the position of this shoulder in the nickel thiocyanate complexes.[37] As the thiocyanate moves from nitrogen (M-NCS) to sulfur (M-SCN) and then to bridged coordinations, a shift of the intense side of the C−N stretching band to the higher wavenumbers was observed by 30−40, 50−70, and 70−120 cm^{-1}, respectively. This observation leads to the assumption that cyanate ion should be oxygen bonded to Ni^{2+} in α-Ni(OH)$_2$ precipitates. Recently, Yang et al. studied the adsorption of cyanate on Ni(100) surfaces with ab initio methods.[38,39] They considered energetics of N- and O-bonded geometries on three different surface sites. Using their assignments, we will demonstrate how the deconvolution of the C−N absorption peak can reveal information about cyanate bonding geometries in α-Ni(OH)$_2$ and Ni−Al LDHs.

Experimental Methods

Powder Synthesis. All chemicals used in this study were reagent grade and used without further purification. Precipitation of nickel hydroxide by urea decomposition was carried out as described previously.[18,19,40] A total of 5.9428 g of $NiCl_2\cdot 6H_2O$ (Fisher Scientific) was dissolved in 190 mL of deionized water and preheated at 90 ± 1 °C; 30.0300 g of urea (Fisher Scientific) was dissolved in 60 mL of deionized water and added to the preheated Ni^{2+} solution. Concentrations of Ni^{2+} and urea in the resulting solution correspond to 0.1 and 2.0 M, respectively. Sample aliquots were withdrawn at various digestion times from the middle of the stirred solution. Precipitates were separated from the mother liquor by an in-line filter, washed three times, and saved for further analysis after drying at 70 °C. A similar procedure was followed for the Ni−Al LDH synthesis employing 0.075 M Ni^{2+} and 0.025 M Al^{3+} (as $AlCl_3\cdot 6H_2O$, Fisher Scientific) solution. These samples from Ni^{2+} and Ni^{2+}−Al^{3+} are referred to as α-[time] and LDH-[time], respectively. α−β transformation was monitored by aging, α-[2 h] and 5% Co^{2+} doped α-[2 h] samples in 6 M KOH for 1 week.[40,41]

(21) Demourgues-Guerlou, L.; Delmas, C. Effect of iron on the electrochemical properties of the nickel hydroxide electrode. *J. Electrochem. Soc.* **1994**, *141* (3), 713−7.
(22) Ehlsissen, K. T.; Delahaye-Vidal, A.; Genin, P.; Figlarz, M.; Willmann, P. Preparation and characterization of turbostratic nickel/aluminum layered double hydroxides for nickel hydroxide electrode applications. *J. Mater. Chem.* **1993**, *3* (8), 883−8.
(23) Indira, L.; Dixit, M.; Kamath, P. V. Electrosynthesis of layered double hydroxides of nickel with trivalent cations. *J. Power Sources* **1994**, *52* (1), 93−7.
(24) Rajamathi, M.; Thomas, G. S.; Kamath, P. V. The many ways of making anionic clays. *Proc. Indian Acad. Sci., Chem. Sci.* **2001**, *113* (5−6), 671−80.
(25) Costantino, U.; Marmottini, F.; Nocchetti, M.; Vivani, R. New synthetic routes to hydrotalcite-like compounds. Characterization and properties of the obtained materials. *Eur. J. Inorg. Chem.* **1998** (10), 1439−46.
(26) Mavis, B. Homogeneous precipitation of nickel hydroxide powders. Ph.D. Thesis, Iowa State University, Ames, IA, 2003.
(27) Shu, X.; Zhang, W.; He, J.; Gao, F.; Zhu, Y. Formation of Ni-Ti-layered double hydroxides using homogeneous precipitation method. *Solid State Sci.* **2006**, *8* (6), 634.
(28) Kloprogge, J. T.; Hickey, L.; Trujillano, R.; Holgado, M.; San Roman, M. S.; Rives, V.; Martens, W. N.; Frost, R. L. Characterization of intercalated Ni/Al hydrotalcites prepared by the partial decomposition of urea. *Cryst. Growth Des.* **2006**, *6* (6), 1533−6.
(29) Vial, S.; Prevot, V.; Forano, C. Novel route for layered double hydroxides preparation by enzymatic decomposition of urea. *J. Phys. Chem. Solids* **2006**, *67* (5−6), 1048.
(30) Li, B.; He, J.; Evans, D. G.; Duan, X. Morphology and size control of Ni-Al layered double hydroxides using chitosan as template. *J. Phys. Chem. Solids* **2006**, *67* (5−6), 1067.
(31) Aggarwal, R. C.; Chandrasekhar, V. Synthesis and structural studies on some diamine complexes of cobalt(II) and nickel(II) cyanates and azides. *Indian J. Chem., Sect. A: Inorg., Bio-inorg., Phys., Theor. Anal.* **1979**, *17A* (4), 361−3.
(32) Dieck, R. L.; Moeller, T. Rare earths. LXXXVI. Isocyanato adducts of lanthanide(III) chlorides and isothiocyanates. *J. Less-Common Metals* **1973**, *33* (3), 355−60.
(33) Quastlerova-Hvastijova, M.; Kohout, J.; Gazo, J. Cyanato copper complexes with organic ligands. VI. Preparation, electronic, and infrared spectra of cyanato copper(II) complexes with aniline derivative ligands. *Z. Anorg. Allg. Chem.* **1973**, *396* (3), 341−52.
(34) Sabatini, A.; Bertini, I. Infrared spectra between 100 and 2500 cm^{-1} of some complex metal cyanates, thiocyanates, and selenocyanates. *Inorg. Chem.* **1965**, *4* (7), 959−61.
(35) Forster, D.; Goodgame, D. M. L. Vibrational spectra of pseudohalide complexes. I. Tetrahedral isocyanate complexes. *J. Chem. Soc.* **1965**, *Jan.*, 262−7.
(36) Tsintsadze, G. V.; Mamulashvili, A. M.; Demchenko, L. P. Products of the reaction of hexamethylenetetramine with cyanates, thiocyanates, and selenocyanates of some metals. *Zh. Neorg. Khim.* **1970**, *15* (1), 276−8.
(37) Carbacho, H.; Ungerer, B.; Contreras, G. Pseudo-octahedral and polymeric complexes of nickel(II) with thiocyanate. *J. Inorg. Nucl. Chem.* **1970**, *32* (2), 579−84.
(38) Yang, H.; Whitten, J. L. Chemisorption of OCN on Ni(100)—an ab initio study. *Surf. Sci.* **1998**, *401* (3), 312−21.
(39) Yang, H.; Whitten, J. L. Reaction and adsorption energetics of CN + O → OCN on nickel. *THEOCHEM* **1999**, *458* (1−2), 131−42.
(40) Mavis, B.; Akinc, M. Homogeneous precipitation of layer double hydroxides. *Key Eng. Mater.* **2004**, 264−268, 41−4.
(41) Mavis, B.; Akinc, M. Three-component layer double hydroxides by urea precipitation: Structural stability and electrochemistry. *J. Power Sources* **2004**, *134* (2), 308−17.

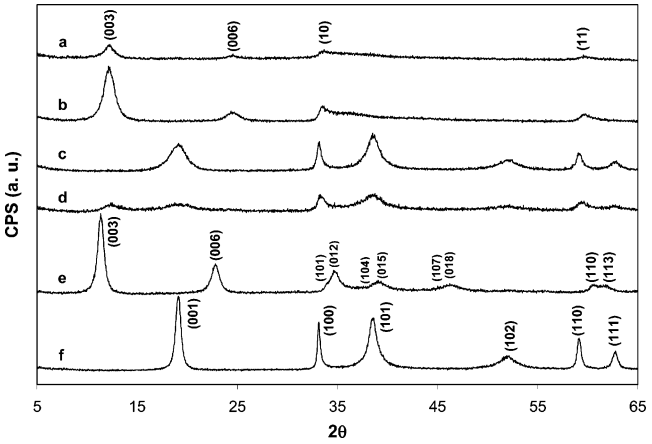

Figure 1. XRD Patterns from (a) α-[2 h] (shaken), (b) α-[2 h] (stirred), (c) α-[2 h] (aged/mostly transformed to β), (d) 5Co-α-[2 h] (aged/partially transformed to β), (e) LDH-[2 h], and (f) β-$Ni(OH)_2$. Each peak in representative patterns from α and β, and LDH is marked with their indices.

Characterization. A powder X-ray diffraction (Scintag X1-365) unit with Cu Kα radiation was used for structural characterization. For crystallite size determinations, instrumental broadening was accounted for using crystalline silicon reference.[42] Turbostratic character of the layers relative to each other was judged by comparing the asymmetric peak between $2\theta = 30°$ and 55°.

Bulk carbon, nitrogen, and hydrogen contents of the precipitated powders were determined using a Perkin-Elmer series II CHNS/O 2400 analyzer. Each analysis represents average of three measurements. Nickel and aluminum contents were determined by atomic absorption spectrometer (Perkin-Elmer, Downers Grove, IL).

FTIR experiments were conducted in transmission mode with KBr pellets containing 0.70−0.75% sample. Spectra from the 4000−400 cm^{-1} range were recorded in a Bomem−Hartmann and Braun-MB 102 unit with 4 cm^{-1} resolution with pure KBr as the reference. Analysis on FTIR and XPS data was carried out using PeakFit (Version 4.11, SYSTAT Software Inc.) software, which is capable of smoothing, background subtraction, and peak deconvolution. In some cases, cyanate peak around 2200 cm^{-1} was deconvoluted to assign specific coordination modes. Relative ratio of integrated peak areas was used to estimate the relative populations of specific modes.

X-ray photoelectron spectra (XPS) were acquired using a Physical Electronics 5500 Multitechnique spectrometer with monochromatic Al and standard Mg/Al sources. Spectra with energy resolution of less than 0.50 eV FWHM were obtained. The photoelectron spectra were calibrated against the adventitious carbon at 285.0 eV.[43]

Also recorded were the FTIR and XPS control spectra for NaOCN, AgOCN, and β-$Ni(OH)_2$ (Aldrich Chemical Co.) and Na_2CO_3 and $NaHCO_3$ (Fisher Scientific). A sample formed by mixing NaOCN and β-$Ni(OH)_2$ (β-OCN) provided information on the possible signatures of adsorption of cyanate on the nickel hydroxide surfaces. Powder morphology was studied with an SEM system (Hitachi S-2460N VP-SEM).

Results

Structure and Size. XRD patterns of several samples are given in Figure 1. All α-[2 h] samples exhibit "turbostratic" α-$Ni(OH)_2$ similar to ones reported by others[3,17,44,45] Interlayer spacing along the *c*-axis that was calculated from the positions of [003] peak were all similar and equal to 7.24 ± 0.02 Å. Random orientation of layers about the *c*-axis in turbostratically disordered phase eliminates the (*hkl*) reflections. Only (00*l*) and (*hk*0) reflections are observed.[46] A similarly small interlayer spacing was also reported by Shu et al., who have prepared Ni−Ti LDHs using urea hydrolysis.[27] The interlayer separation calculated for the LDH-[2 h] was 7.80 ± 0.02 Å in agreement with the literature values.[47] XRD pattern of β-$Ni(OH)_2$. is presented in the Figure 1 for comparison (trace f). Recently, Thomas and Vishnu Kamath have reported that in calculation of crystallite sizes of layered hydroxides by the application of Scherrer formula; line broadening caused by structural disorder (stacking faults, interstratification, and turbostratic disorder) has to be discounted for good estimates.[48] Bearing this in mind, the evolution of calculated crystallite sizes with digestion time was approached cautiously. Nevertheless, it is safe to say that the crystallite sizes remain within the order of magnitude (along *c*-axis 5.6 to 7.6 nm for 50 min and 36 h of digestion, respectively) throughout the investigated digestion times. From SEM micrographs, it can be inferred that the sizes of particles after 2 h of digestion are on the order of several microns. Higher magnifications reveal that these micron-sized particles are the agglomerates of sheet-like primary crystallites. This implies the dominance of an agglomerative growth mechanism.[18,26,41]

Chemical Composition. Presence of cyanate ion in urea precipitated α-$Ni(OH)_2$ and Ni/Al LDH powders was reported earlier.[18,19,40,41] The formula, $Ni(OH)_{1.45}(OCN)_{0.47}(HCO_3)_{0.05}Cl_{0.02}\cdot 0.59H_2O$, which was inferred from predictive modeling studies in combination with elemental analysis, offers a reasonable presentation of the chemical composition of the α-[2 h] precipitate. Consistent with the predictions, cyanates were the dominant interlayer anions.[18] Based on the elemental analysis results, the formula for Ni−Al LDH (LDH-[2 h]) with the synthesis ratio of Ni/Al = 3 can be described as $Ni_{0.77}Al_{0.18}(OH)_{1.84}(OCN)_{0.08}(CO_3)_{0.08}\cdot 0.61H_2O$.[41] The observed Ni/Al ratio (0.77/0.18 ≈ 4.3) is slightly larger from that in the starting solution. The lack of coincidence between the initial ratio of cations in the solution and the ratio in the final solid is, however, rather common[27] and may be ascribed to a preferential precipitation of one of the cations as hydroxide and/or complexation reactions or error during measurement. Here, possibly the precipitation of colloidal $Al(OH)_3$ or formation of aluminum hydroxide complexes

(42) Boulc'h, F.; Schouler, M.-C.; Donnadieu, P.; Chaix, J.-M.; Djurado, E. Domain size distribution of Y-TZP nanoparticles using XRD and HRTEM. *Image Anal. Stereology* **2001**, *20* (3), 157−61.
(43) Swift, P. Adventitious carbon−the panacea for energy referencing? *Surf. Interface Anal.* **1982**, *4* (2), 47−51.
(44) Delahaye-Vidal, A.; Figlarz, M. Textural and structural studies on nickel hydroxide electrodes. II. Turbostratic nickel(II) hydroxide submitted to electrochemical redox cycling. *J. Appl. Electrochem.* **1987**, *17* (3), 589−99.
(45) Portemer, F.; Delahaye-Vidal, A.; Figlarz, M. Characterization of active material deposited at the nickel hydroxide electrode by electrochemical impregnation. *J. Electrochem. Soc.* **1992**, *139* (3), 671−8.
(46) Prakash, A. S.; Kamath, P. V.; Hegde, M. S. Synthesis and characterization of the layered double hydroxides of Mg with Cr. *Mater. Res. Bull.* **2000**, *35* (13), 2189−97.
(47) Wang, C. Y.; Zhong, S.; Konstantinov, K.; Walter, G.; Liu, H. K. Structural study of Al-substituted nickel hydroxide. *Solid State Ionics* **2002**, *148* (3,4), 503−8.
(48) Thomas, G. S.; Vishnu Kamath, P. Line broadening in the PXRD patterns of layered hydroxides: the relative effects of crystallite size and structural disorder. *J. Chem. Sci.* **2006**, *118* (1), 127.

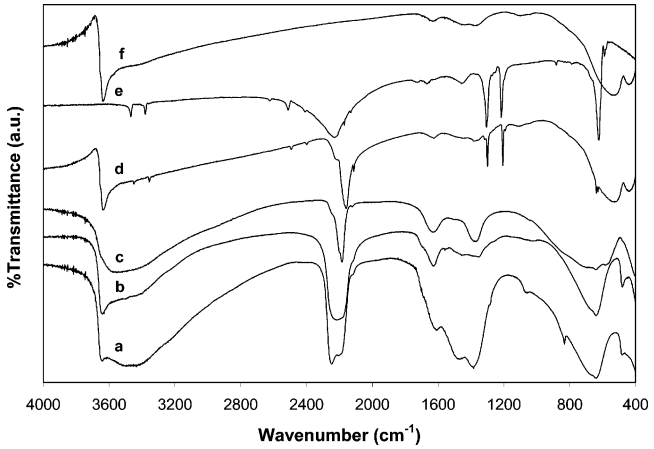

Figure 2. FTIR spectra of (a) α-[2 h] (shaken), (b) α-[2 h] (stirred), (c) LDH-[2 h], (d) a mixture of NaOCN and β-Ni(OH)$_2$ (Aldrich Chemical Co.), (e) NaOCN, and (f) β-Ni(OH)$_2$.

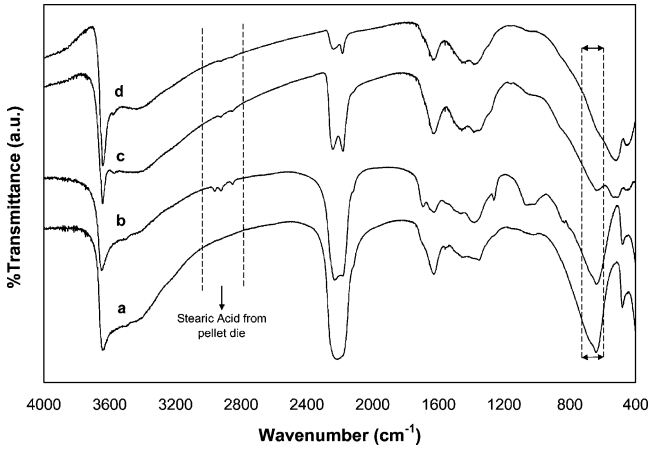

Figure 3. FTIR spectra of (a) α-[2 h] (stirred), (b) α-[36 h] (stirred/dried in a vacuum oven at 70 °C for 12 h), (c) 5Co-α-[2 h] (aged/partially transformed to β), and (d) α-[2 h] (aged/mostly transformed to β).

causes this discrepancy. It should be noted that the amount of cyanate in the Ni−Al LDH is significantly lower than that in α-Ni(OH)$_2$.

FTIR Spectra. Particular significance of cyanate ion in precipitation of α-Ni(OH)$_2$ was reported earlier.[18,19,40] Figure 2 shows the FTIR spectra taken from α-[2 h] as compared to that of β-Ni(OH)$_2$ and LDH-[2 h] and illustrates the significant differences among the three. In addition, spectra from NaOCN and a mixture of NaOCN and β-Ni(OH)$_2$ (β-OCN) is also given in Figure 2.

The sharp peak around 2200 cm^{-1} has been assigned to C−N stretch of OCN^- in nickel hydroxide precipitated with urea.[11,14,17,27] This band normally manifests itself as a broad band in the NaOCN spectrum (Figure 2e), whereas it shows different profiles upon adsorption and/or intercalation of cyanate as can be observed from Figure 2a−d. For instance, while it has a high wavenumber shoulder for both LDH or β-OCN, the shoulder seems to appear at low wavenumbers in α. Unique "splitting and shoulder" features observed in different samples imply that the origin or configuration of these species may be different.

Various metal−NCO complexes and free OCN^- ion have been observed to have sharp peaks at ≈620 and 630 cm^{-1}, respectively,[35,36,49] and they provide distinct signatures for labeling of cyanate-containing compounds.[50] Throughout our studies, when the OCN^- was missing (in α phases precipitated by heterogeneous precipitation) or diminishing during transformation to β phase (Figure 3), the sharp protrusion at 630−640 cm^{-1} disappeared.[26] This missing feature became apparent as a shoulder upon removal of the carbonaceous intercalation species or upon vacuum drying proving that the 2200 cm^{-1} feature is indeed due to cyanate. Relatively weaker pseudo-symmetric stretching of C−O bond of cyanate in metal cyanate complexes that was reported by Forster et al.[35] and Tsintsadze et al.[36] was observed at 1330 and 1318 cm^{-1}, respectively. A considerable shift (by ≈100 cm^{-1} with respect to the reference compounds' at ≈1200 cm^{-1}) in this mode toward high wavenumbers is generally taken as evidence of nitrogen bonding to the metal ion.[36] While these bands can be observed in the β-OCN or NaOCN spectra, they seem to vanish in α and LDH spectra. This brings the question whether if there are different possibilities besides coordination through nitrogen. Obviously, coordination modes of cyanate in the α-Ni(OH)$_2$ and Ni−Al LDHs are far from being well understood and require further study.

Spectral Analysis. Representative deconvolutions of the cyanate peak (≈2200 cm^{-1}) in α-[2 h] and LDH-[2 h] samples are given in Figure 4. Results imply that cyanate has more than one coordination mode. Although not quantitative, the integrated area under a peak is related to its content in the sample. In Figure 5A,B, the change in relative area under the deconvoluted peaks (% area) is given with respect to time for α-[time] and LDH-[time].

Analysis of the data for α-[time] samples indicates that while 2184, 2158, and 2117 cm^{-1} peak intensities decrease, 2214 and 2250 cm^{-1} peaks emerge and increase in intensity. Another interesting trend is that 2214 cm^{-1} seems to be compensated by 2250 cm^{-1} until a break point, which is followed by a decrease in 2250 cm^{-1}. Interestingly, the 2182 cm^{-1} peak dominates throughout the entire digestion in LDH-[time] samples. Using the analogy drawn between nickel thiocyanate and nickel cyanate complexes,[37] one may state that the cyanate that is dominantly nitrogen bonded (i.e., isocyanate: -NCO) in the initial stages, changes to an oxygen bonded (i.e., cyanate: -OCN) or to bridging coordination (bonded through N and O simultaneously).

Surface chemical analysis of the precipitates by XPS at various digestion times gives an accurate representation of instantaneous composition of the growing particle and may be related to bulk chemical analysis of the samples reported previously.[18] In addition, the chemical environment of the element can be deduced by examination of its chemical shifts. Results of typical deconvolutions are given in Figure 6.

Results of XP spectra deconvolutions are given in the Supporting Information. Briefly, all reference spectra show good agreement with literature data.[51−53] There is almost 1 eV difference in the binding energies observed for C−N peak positions in C1s spectra of α-[time] and LDH-[time] samples.

(49) Nakamoto, K. *Infrared and Raman Spectra of Inorganic and Coordination Compounds, Part B: Applications in Coordination, Organometallic, and Bioinorganic Chemistry*, 5th ed.; John Wiley & Sons: New York, 1997; p 384.

(50) Conrad, D. W.; Patterson, C. H., Jr. Compounds labeled with cyanate or thiocyanate metal complexes for detection by infrared spectroscopy and analytical applications. U.S. Patent 940736, 1998.

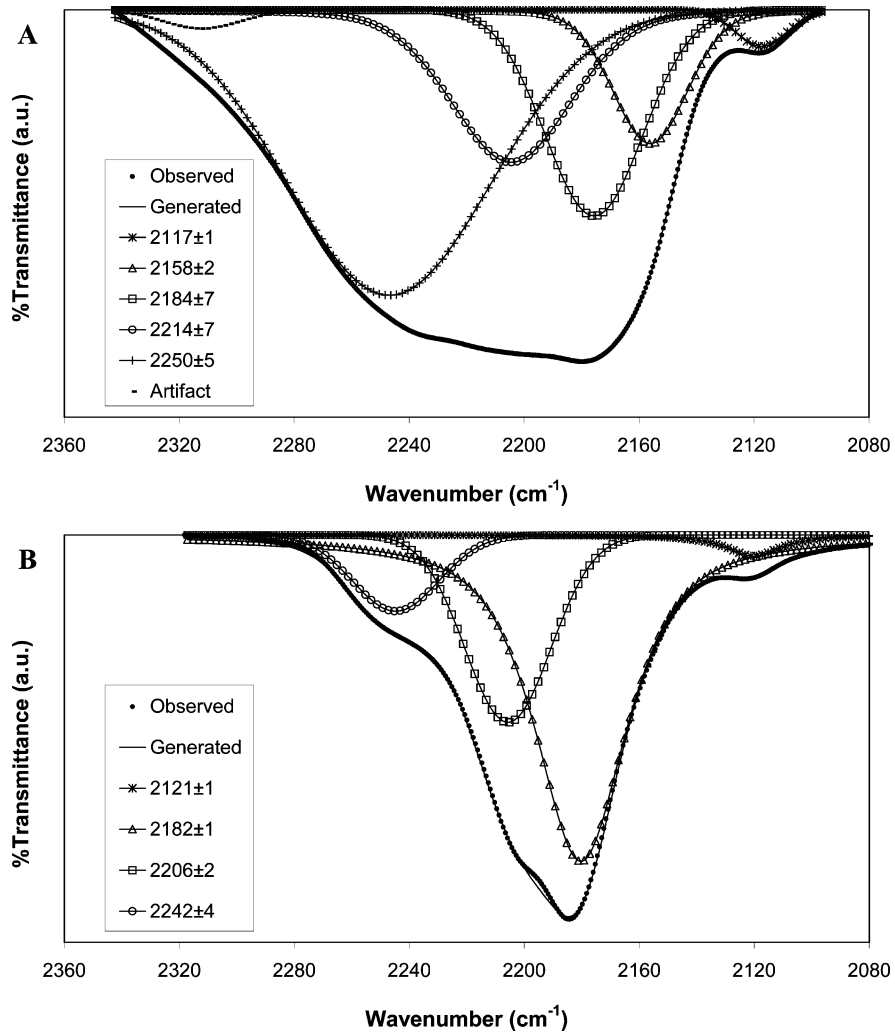

Figure 4. Representative deconvolution of the ≈2200 cm^{-1} region in (A) α-[2 h] and (B) LDH-[2 h] samples.

Such a difference could be an indication of a considerable change in the electronic charge residing on carbon atom. This observation is in agreement with the observed differences noted in FTIR spectra of α-[time] and LDH-[time] samples.

Bulk chemical analysis reported previously showed a decrease in nitrogen content with digestion time.[18,19] This was in agreement with kinetic simulations that predicted a decrease in the concentration of nickel cyanate complexes, implying that interlayer chemistry of the crystallites changes with digestion time. Since XRD results suggest that the growth mechanism is mainly by agglomeration of the primary crystallites,[18] crystallites formed at the later stages of precipitation are expected to have a different composition with respect to cyanate. Figure 7 compares the variation of nitrogen concentration as a function of time by bulk (wet chemical) and surface (XPS) analyses. All XPS data was normalized against a maximum peak intensity from C1s (cyanate) at 287.6 eV. Because of the nature of the two analytical techniques, only trends in the change in nitrogen content with time should be considered.[54] As expected, nitrogen (i.e., cyanate) content decreases at a much faster rate along the cross section of a particle.

Discussion

FTIR peak centered at around 2200 cm^{-1} showed a distinct split character. Literature is rather limited on the nature of the splitting of this peak. In most cases it was not mentioned or noticed. For instance, Tsintsadze et al. studied the coordination compounds of metals cyanates (nickel included) with urotropine. They reported a peak around 2230 cm^{-1} but never mentioned a shoulder.[36] In one instance, a shoulder at 2237 cm^{-1} for a sharp peak at 2186 cm^{-1} was noted.[35] As demonstrated above, in an ionic crystal lattice like α-Ni-$(OH)_2$ or Ni−Al LDH, one can observe up to four peaks in the same region besides 2186 cm^{-1}.

Peak splitting in an FTIR spectrum can be attributed to a loss of symmetry of anion in the solid state[35] and changes in electronegativity, oxidation number, and coordination number of the metal.[55] It is probable that a combination of

(51) Atzei, D.; De Filippo, D.; Rossi, A.; Caminiti, R. X-ray photoelectron spectra of dinitrogen chelating ligands with some transition metals. *Spectrochim. Acta, Part A* **1993**, *49A* (12), 1779−85.
(52) Owens, F. J.; Sharma, J. XPS measurement and molecular orbital calculation of valence band electronic structure of sodium cyanate. *Chem. Phys. Lett.* **1980**, *74* (1), 72−4.
(53) D'Agnano, A.; Gargano, M.; Malitesta, C.; Ravasio, N.; Sabbatini, L. X-ray photoelectron spectroscopy insight into the coordination modes of cyanate in copper(II) complexes. *J. Electron Spectrosc. Relat. Phenom.* **1991**, *53* (4), 213−24.
(54) Skoog, D. A.; West, D. M.; Holler, F. J. *Fundamentals of Analytical Chemistry*, 7th ed.; Harcourt Inc.: Orlando, FL, 1997.

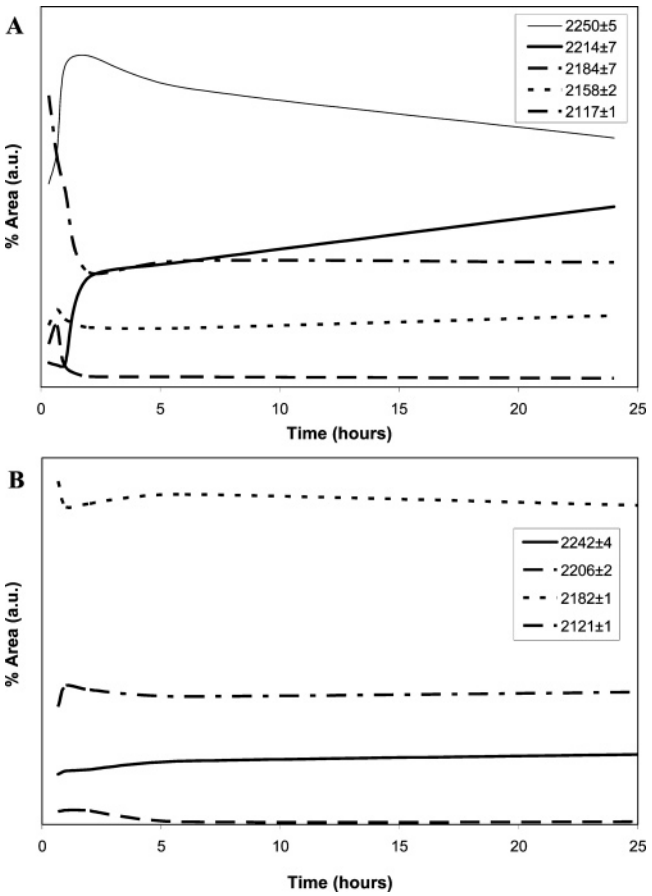

Figure 5. Relative integrated area (% area) under the deconvolved peaks from ≈2200 cm^{-1} band with respect to time for (A) α-[time] and (B) LDH-[time] samples. Peak positions are averages of positions observed with respect to time.

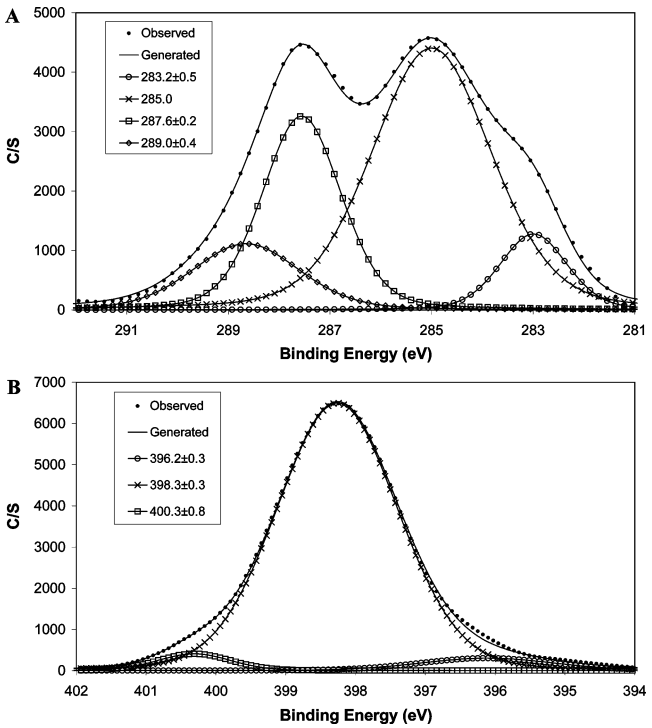

Figure 6. Typical peak fitting for the (A) C1s and (B) N1s spectra of the α-[2 h].

these factors resulted in the peak splitting observed in this study. Ben-Efraim[56] noted that organic molecules of isocyanate (N-coordinated) and cyanate (O-coordinated) are characterized by strong bands at 2290−2240 and 2280−2240 cm^{-1}, respectively, independent of the alkyl constituent they are associated with. Isocyanate absorption was usually a singlet with signs of broadening from Fermi resonance (FR) effect, whereas cyanate was slightly asymmetric or split into a doublet due to the same effect. This is in support of a proposal that cyanate can be coordinated through its oxygen as well as its nitrogen in a layered hydroxide structure.

In a previous study,[18] we showed accumulation of cyanate ion and subsequent formation of nickel cyanate complexes during the first 2 h of digestion. The role of cyanate anion in triggering the crystallization along the *c*-axis was illustrated here. From the peak-shape profiles, it can be proposed that the coordination of cyanate might be changing from nitrogen-bonded (as in tetrahedral isocyanate complexes[35]) to oxygen-bonded, bridging, or hydrogen-bonded free anion.[53]

It may not be safe to relate all the information from the FTIR and XP spectra only to cyanate ions intercalated within the interlayer spaces of the particles. Part of the signals could be attributed to cyanate adsorbed on the surface of the particles and the bonding modes of the adsorbed species may be different from those of the intercalated species. The CN absorption in the β-OCN sample (physical mixture) is observed at a significantly low wavenumber (≈ 2164 cm^{-1}). If the similarly low wavenumber absorptions from the precipitates of this study could be attributed to surface adsorbed species, it can be concluded that the population of the surface adsorbed species (i.e., low wavenumber modes) remains relatively low and constant as compared to that of high wavenumber modes. In support of the above argument, BET surface areas of the powders do not change significantly with the prolonged digestion times. This suggests that the available surfaces of the micron-sized secondary particles remain at a constant level.[9,10]

Carbacho et al. studied complexes of Ni^{2+} with thiocyanate to distinguish between N- versus S- coordination of the thiocyanate.[37] They reported a shift of the intense side of this stretch to higher wavenumbers by 30−40 cm^{-1} for M-NCS, 50−70 cm^{-1} for M-SCN, and 70−120 cm^{-1} for bridged coordination as compared to free ion. A very intense peak was reported along with a shoulder in almost all coordination modes. In addition, these shoulders changed their positions from high wavenumbers to low wavenumbers as the coordination mode changed from nitrogen-bonded to sulfur-bonded. Despite the inherent differences in the chemistries, an analogy can be drawn between thiocyanate and cyanate complexes of Ni^{2+}. It was claimed that since the steric requirements for an angular M-SCN linkage would be greater than for a linear M-NCS bonding, the latter would be preferred with bulky ligands. On the other hand, the additional stability provided by the interaction of d-electrons of the metal with the empty antibonding orbitals localized on

(55) Ahlijah, G. E. B. Y.; Mooney, E. F. Attenuated total reflection spectra of polyatomic inorganic anions. II. Nitrogen-containing anions. *Spectrochim. Acta, Part A* **1969**, *25* (3), 619−27.
(56) Ben-Efraim, D. A. Detection and determination of cyanates, isocyanates, isothiocyanates, and thiocyanates. *Chem. Cyanates Their Thio Deriv.* **1977**, *1*, 191−236.

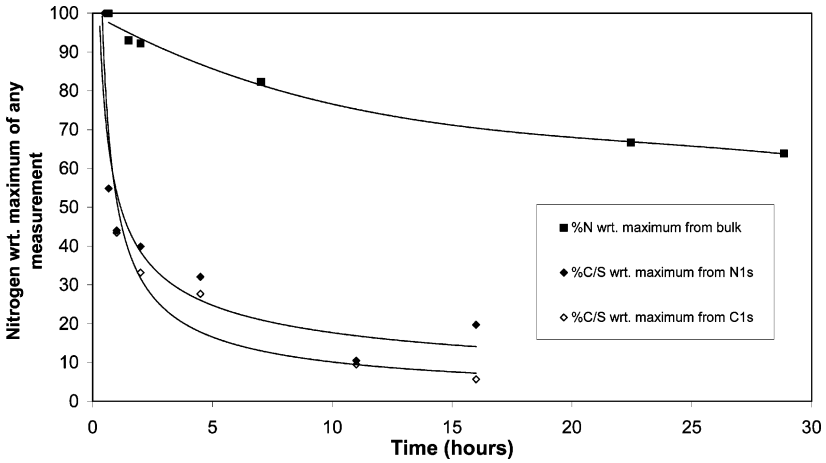

Figure 7. Qualitative comparison of elemental nitrogen analysis from bulk with analyses from N1s and C1s XP spectra. Note that every data point within one set is normalized with the maximum among that set. Solid lines represent the trend in data.

sulfur (π bonding) could help the electronic factors to dominate. Although this effect is frequently reported for thiocyanates, the case is not always the same for cyanates.[49,53] D'Agnano et al. noted that all cyanate complexes of first-row transition metals had been claimed to be N-bonded, despite the fact that first principles calculations had pointed out equal densities existing on nitrogen and oxygen.[53] Although the majority of the literature suggests coordination through nitrogen,[35,36,49,51,57] the existence of bridging coordinations was also reported.[53,58] In addition, spectral analysis in this study suggests that there can be up to five different peaks in the region. Considering the analogy between thiocyanate and cyanate, a plausible explanation can be developed for the changes observed in FTIR by taking steric and/or electronic contributions into the consideration. Initially, steric factors must be preventing the coordination of cyanate through oxygen. With increasing digestion times however, the additional peaks, positions of which favors either oxygen or bridging coordinations, starts to emerge indicating that the electronic factors might become significant.

Recently, Yang and Whitten have studied the chemisorption of cyanate on Ni(100) using the ab initio many-electron embedding theory.[38,39] They compare their result and find good agreement with the few experimental data, which was cited above. The agreement between our results and their calculations is remarkable and supports our model.

We had noted that the $\approx$2200 cm^{-1} region of the α-[time] spectra can be represented by five modes, namely (in accordance with notation of Yang and Whitten):

(i) 2250 $\pm$ 5 cm^{-1}: O-bonded cyanate at "atop" (unidentate on top of nickel atom),

(ii) 2214 $\pm$ 7 cm^{-1}: O-bonded Cyanate at "4-fold",

(iii) 2184 $\pm$ 7 cm^{-1}: N-bonded isocyanate at "atop",

(iv) 2158 $\pm$ 2 cm^{-1}: N-bonded isocyanate at "bridge" (bidendate between two nickel atoms) or "4-fold",

(v) 2117 $\pm$ 1 cm^{-1}: observation of "% Area vs time" plots for α-[time] reveals that trend in population of these species follows the one of 2158 cm^{-1} species.

A similar analysis for LDH-[time] leads to the following assignments:

(i) 2242 $\pm$ 4 cm^{-1}: O-bonded Cyanate-O at "atop",

(ii) 2206 $\pm$ 2 cm^{-1}: O-bonded Cyanate at "4-fold",

(iii) 2182 $\pm$ 1 cm^{-1}: N-bonded isocyanate at "atop",

(iv) 2121 $\pm$ 1 cm^{-1}: similar to 2117 cm^{-1} observed for α-[time] samples.

All N-bonded isocyanate species were found to be more stable than O-bonded cyanate by about 15 kcal/mol in respective sites.

Based on the above discussion and assignments, it is reasonable to conclude that the cyanate coordination changes from N-bonded to O-bonded with digestion time as 2214 and 2250 cm^{-1} peaks (O-bonded) dominate the 2184, 2158, and 2117 cm^{-1} peaks (N-bonded). LDH-[time] shows the domination of N-bonded species throughout the entire digestion. This difference in coordination appears to be the primary factor for the difference in the relative stabilities of LDH and α-[time] against transformation to β phase.[40,41]

One can discuss whether the Ni(100) can be assumed similar to a "defective" brucite-type layer, which is generally assumed[1,59] and had been confirmed in our previous study[18] for α-Ni(OH)$_2$. Figure 8 depicts four of the many possibilities of these defect sites. Examination of the defect sites indicates

(57) Bron, M.; Holze, R. Cyanate and thiocyanate adsorption at copper and gold electrodes as probed by in situ infrared and surface-enhanced raman spectroscopy. *J. Electroanal. Chem.* **1995**, *385* (1), 105−13.

(58) Le Borgne, C.; Chabanel, M. Vibrational study of ionic association in polar aprotic solvents. Isocyanate complexes of non-transition-metal ions. *J. Mol. Liq.* **1997**, *73* (74), 171−8.

(59) Kamath, P. V.; Dixit, M.; Indira, L.; Shukla, A. K.; Kumar, V. G.; Munichandraiah, N. Stabilized α-Ni(OH)$_2$ as electrode material for alkaline secondary cells. *J. Electrochem. Soc.* **1994**, *141* (11), 2956−9.

(60) Whelan, C. M.; Neubauer, R.; Borgmann, D.; Denecke, R.; Steinruck, H.-P. A fast X-ray photoelectron spectroscopy study of the adsorption and temperature-dependent decomposition of propene on Ni(100). *J. Chem. Phys.* **2001**, *115* (17), 8133−40.

(61) Weckhuysen, B. M.; Rosynek, M. P.; Lunsford, J. H. Characterization of surface carbon formed during the conversion of methane to benzene over Mo/HZSM-5 catalysts. *Catal. Lett.* **1998**, *52* (1, 2), 31−6.

(62) Jing, S.-Y.; Choi, C. K.; Lee, H.-J. A study on the formation and characteristics of the organic-inorganic material with low dielectric constant deposited by high density plasma chemical vapor deposition. *J. Korean Phys. Soc.* **2001**, *39* (Suppl.), S302−5.

(63) Bartlett, B.; Valdisera, J. M.; Russell, J. N., Jr. A comparison of the surface chemistry of phenyl cyanate and phenol on Al(111). *Surf. Sci.* **1999**, *442* (2), 265−76.

(64) Matienzo, J.; Yin, L. I.; Grim, S. O.; Swartz, W. E., Jr. X-ray photoelectron spectroscopy of nickel compounds. *Inorg. Chem.* **1973**, *12* (12), 2762−9.

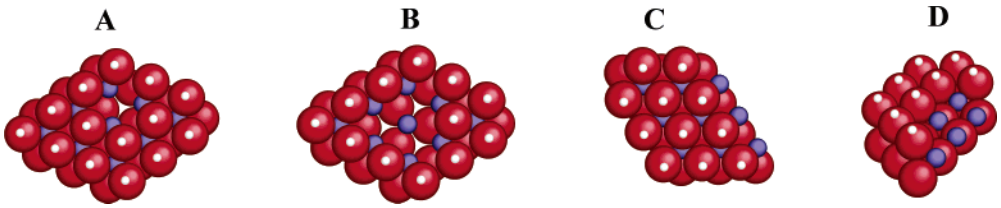

Figure 8. Defect possibilities in α structures: missing (A) one; (B) three hydroxyl ions from the layer; (C) broken crystallite side, which might permit an uninterrupted exposure of nickel ions; and (D) broken crystallite side with additional defects in the adjacent layer hydroxyl positions.

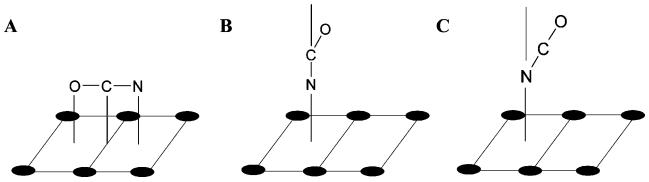

Figure 9. (A) Equilibrium geometry for the side-on bonded OCN. The carbon atom is adsorbed above the bridge site. E_{ads} relative to OCN at infinite separation is 84 kcal/mol. Note this geometry brings carbon to the proximity of nickel. End-on N-bonded OCN at 4-fold site with tilt between (B) the O−C bond and the surface normal and (C) the O−C−N axis and the surface normal. Reproduced from ref 38.

that the dominant modes are generally at "atop" sites, which in fact corresponds to a "grafted" interlayer species, for O-bonded cyanate and N-bonded isocyanates. The interlayer space observed in α phase (7.24 ± 0.02 Å) was relatively lower than that in LDH (7.80 ± 0.02 Å). Although it is plausible that the α phase might not be pure but interstratified with β phase; envisioning of a "grafted" cyanate or isocyanate (i.e., replacement of the layer hydroxyls with the nitrogen or the oxygen of the grafting cyanate) can also justify the relatively low interlayer spacing observed in the α phase.

Broken edges of crystallites illustrate the appearance of the other modes as shown in Figure 8C. Energetics of an OCN tilted away from the surface normal and side-on geometry was also tackled by Yang and Whitten.[38] Three of the geometries studied are shown in Figure 9. The adsorption energy reported for side-on geometry was comparable to that of all O-bonded cyanate species, while significantly smaller than for the N-bonded isocyanate species. The stretching frequencies calculated were 2057 and 1510 cm^{-1} for C−N and C−O, respectively. Cyano complexes ($[M(CN)_4]^{2-}$) or fulminato complexes ($[M(CNO)_4]^{2-}$) were reported to have absorptions between ≈2110 and 2190 cm^{-1} and are assigned to C−N stretches.[49] Hence the modes observed at 2117 and 2121 cm^{-1} for α and LDH samples can be assigned to side-on geometry that is closely related to what is depicted in Figure 9.

Although tilting C−O or the O−C−N axis away from the surface was reported to be destabilizing the system, the adsorption energies for a tilt angle of ≈30° and ≈60° for CO and OCN tilts were all similar and close to 82 kcal/mol. Thus, the scatter in our data can be explained by different modes that are energetically equivalent. The existence of XPS peak in our samples, which could be assigned to carbidic carbon (direct Ni−C bond), lends additional support for the existence of side-on geometry.

Dipole moment calculations indicate that both O-bonded and N-bonded cyanates are largely ionic. About 0.8 and 0.7 electrons are transferred to O-bonded and N-bonded isocyanate, respectively, from surface nickel atoms. A very striking observation is that the carbon atom was much more positive (more than twice) in the N-bonded than in the O-bonded structure. This was clearly demonstrated in the C1s peak of XPS. Especially in the case of LDH sample (predominantly N-bonded), an increase of about 1 eV was seen as compared to that of α phase, which was dominantly O-bonded at long digestion times.

Kinetic simulations predicted that bicarbonate ion is the dominant carbonaceous species in the pH temperature range investigated. Therefore, intercalation or adsorption by unidentate coordination is expected over bidentate coordination. However, for the conditions under which anion concentrations remain low (low pH and low supersaturation was observed and predicted[18,19]), charge neutrality requirement may force bicarbonate into bidentate or bridging coordination.[49] The low interlayer distance calculated from XRD data supports the assertion that, since there is not enough space between the layers, conditions may enforce bidentate carbonate adsorption or intercalation.

In our previous paper, the results of urea decomposition simulations indicated that there is a crossover point between the third and fourth hour, where the cyanate and bicarbonate concentrations become the same and beyond which bicarbonate is the dominant species.[18] In light of foregoing discussions, the following nucleation mechanism may be offered. In the initial stages of urea decomposition, the lack of sufficient bicarbonate leads to formation of nickel hydroxide clusters along with nickel cyanate species as the building blocks of the layered structure (N-bonded isocyanate grafts). With time, the instantaneous concentration of cyanate decreases. This decrease is balanced by the increasing bicarbonate levels. However, the supersaturation level decreases with the decreasing metal ion concentrations (constant pH).[18] At this stage "electronic factors: and "charge neutrality" necessitates the coordination of cyanate to change to include O-bonded cyanate (this mode donates more electrons although energetically less stable) as well as the incorporation of bicarbonate in the α phase precipitation. Since the initial pH of the Ni−Al-containing LDH mother liquors is low, a higher decomposition rate of urea is predicted. With these high levels of anion production N-bonded isocyanate coordination remains practically unaltered in LDHs. Although it is difficult to predict what might be happening during the growth of the particles with the available data, it is clear that as concentration of cyanate decreases with time, its role is diminished in the growth process.

Conclusions

Analysis of FTIR data combined with XPS results showed that cyanate species exhibit different bond geometries in α-$Ni(OH)_2$ and Ni/Al LDHs. Assignments for the peaks observed under the cyanate absorption at $\approx$2200 cm^{-1} showed that, with increasing digestion time, cyanate changed from N-bonded to O-bonded end-on geometries in α phase precipitation, whereas it remained predominantly as N-bonded in Ni/Al LDHs. The low supersaturation conditions served by the urea decomposition promote the oxygen coordinated cyanate in the later stages. XPS results indicated a higher positive charge on carbon of cyanate in N-bonded species, which complements FTIR results.

Acknowledgment. This manuscript has been authored by Iowa State University of Science and Technology under Contract W-7405-ENG-82 with the U.S. Department of Energy. The authors thank Drs. Andy Thom and Matt Kramer for valuable discussions and James W. Anderegg for collecting and interpreting XPS data. B.M. furthermore acknowledges the financial support from Catron Fellowship.

Supporting Information Available: A table showing peak positions and assignments in C1s and N1s spectra. This material is available free of charge via the Internet at http://pubs.acs.org.

CM0528835